Electrical Characteristics of Al/Polyindole Schottky Barrier Diodes. I. Temperature Dependence

Seckin Altindal,[1] Bekir Sari,[2] H. Ibrahim Unal,[2] Nihan Yavas[2]

[1]*Department of Chemical Engineering, Faculty of Engineering and Architecture, Gazi University, Ankara 06500, Turkey*
[2]*Polymers Group, Department of Chemistry, Faculty of Science, Gazi University, Ankara 06500, Turkey*

Received 15 December 2008; accepted 2 March 2009
DOI 10.1002/app.30380
Published online 1 May 2009 in Wiley InterScience (www.interscience.wiley.com).

ABSTRACT: In this study, the forward and reverse bias current–voltage (*I–V*), capacitance–voltage (*C–V*), and conductance–voltage (G/ω–*V*) characteristics of Al/polyindole (Al/PIN) Schottky barrier diodes (SBDs) were studied over a wide temperature range of 140–400 K. Zero-bias barrier height $\Phi_{B0}(I–V)$, ideality factor (*n*), ac electrical conductivity (σ_{ac}), and activation energy (E_a), determined by using thermionic emission (TE) theory, were shown fairly large temperature dispersion especially at lower temperatures due to surface states and series resistance of Al/PIN SBD. *I–V* characteristics of the Al/PIN SBDs showed an almost rectification behavior, but the reverse bias saturation current (I_0) and *n* were observed to be high. This high value of *n* has been attributed to the particular distribution of barrier heights due to barrier height inhomogeneities and interface states that present at the Al/PIN interface. The conductivity data obtained from $G/\omega V$ measurements over a wide temperature range were fitted to the Arrhenius and Mott equations and observed linear behaviors for σ_{ac} vs. $1/T$ and ln σ_{ac} vs. $1/T^{1/4}$ graphs, respectively. The Mott parameters of T_0 and K_0 values were determined from the slope and intercept of the straight line as 3.8×10^7 and 1.08×10^7 Scm^{-1} K$^{1/2}$, respectively. Assuming a value of 6×10^{12} s^{-1} for ν_0, the decay length α^{-1} and the density states at the Fermi energy level, $N(E_F)$ are estimated to be 8.74 Å and 1.27×10^{20} eV^{-1}cm^{-3}, respectively. © 2009 Wiley Periodicals, Inc. J Appl Polym Sci 113: 2955–2961, 2009

Key words: Al/PIN Schottky barrier diodes; barrier height; activation energy; temperature dependence; *I–V* and *C–V* characteristics

INTRODUCTION

Semiconductor polymers have attracted a great deal of interest in the past decade and they could be used as active components in the electronic devices due to their excellent electrical characteristics. These devices include field effect transistors, Schottky barrier diodes (SBDs), light emitting diodes and polymeric voltaic cells (PVCs), etc. The performance and reliability of these devices depend on various parameters such as process of fabrication, barrier height between metal and polymer, density of surface states distribution at interface, device temperature and voltage; and thermal and mechanical stability of the semiconductor polymer used.

There are currently a vast number of reports of experimental studies on metal/semiconductor polymer SBDs,[1–12] but very limited experimental information is available on their temperature-dependent electrical characteristics in the literature. Because the analysis of electrical characteristics of these devices measured only at room temperature does not give detailed information about their conduction process and interface characteristics, it is necessary to determine the main diode parameters over a wide temperature range at metal/semiconductor or metal/polymer SBDs to better interpret and understand the nature of barrier and current-conduction mechanism.

Therefore, in this study, to better interpret the experimentally observed diode parameters such as barrier height $\Phi_{B0}(I–V)$, ideality factor (*n*), ac electrical conductivity (σ_{ac}), and activation energy (E_a) determined from *I–V*, *C–V*, and G/ω–*V* measurements were investigated. The electrical characteristics of Al/polyindole (Al/PIN)-SBDs have been studied over a wide temperature range of 140–400 K. Furthermore, the Mott parameters of T_0, K_0, and the density states at the Fermi energy level $N(E_F)$ were also determined. Frequency dependent electrical characteristics of Al/PIN SBDs are also under our investigation and will be published soon, as the second part of the study.

Correspondence to: H. I. Unal (hiunal@gazi.edu.tr).
Contract grant sponsor: Gazi University; contract grant number: FEF 05/2006-45.

© 2009 Wiley Periodicals, Inc.

EXPERIMENTAL

Materials

Analytical grade indole, anhydrous ferric chloride ($FeCl_3$) and chloroform ($CHCl_3$) were purchased from Aldrich and used as received.

Synthesis of polyindole

PIN was chemically synthesized in a nonaqueous medium ($CHCl_3$) under a nitrogen atmosphere using $FeCl_3$ as an oxidizing agent at 15°C for 5 h, taking the ratio of $FeCl_3$ to indole as 3 : 1. Crude PIN was washed with distilled water until the filtrate was clear, dried in a vacuum oven ($P = 15$ mm Hg) at 70°C for 24 h, recovered with 85% yield and used for fabrication of SBDs.

Fabrication of (Al/PIN) SBDs

The Al/PIN SBDs were fabricated by using PIN having thickness of 1.0 mm and diameter of 1.0 cm. High purity (99.999 %) silver (Ag) with a thickness of ~ 2000 Å was thermally evaporated from the tungsten filament onto the whole backside of PIN pellet at a pressure of $\sim 2 \times 10^{-6}$ mmHg. The ohmic contacts were prepared by sintering the evaporated Ag back contact at 450°C for 30 min under dry nitrogen flow at a rate of 2 L/min. This process served to sinter Ag on the upper surface of the PIN pellet. After making ohmic contact, the Schotky (rectifier) contacts formed by evaporation of 2000 Å thick Al dots of ~1.0 mm diameter onto PIN pellet under vacuum. The metal thickness layer and the deposition rates were monitored with the help of quartz crystal thickness monitor. In this way, Al/PIN SBDs were fabricated on PIN pellets.

The electrical characteristics of the Al/PIN SBDs were investigated using I–V, C–V, and G/ω–V measurements under both reverse and forward bias in the wide temperature range of 140–400 K. The I–V measurements were performed by using a Keithley 220 current source and a Keithley 614 electrometer. The C–V and G/ω–V characteristics were performed at 500 kHz by using HP 4192A LF impedance analyzer (5 Hz–13 MHz). The sample temperature was always monitored by means of a Cu–constantan thermocouple and a Lakeshore 321 autotuning temperature controller with sensitivity better than ±0.1 K. All the measurements were carried out with the help of a microcomputer through an IEEE-488 ac/dc converter card.

RESULTS AND DISCUSSION

The temperature dependence of I–V characteristics

A number of Al/PIN SBDs were fabricated and basic electrical parameters mentioned above calculated for each of them. Because all of those diodes fabricated were exhibited the same basic electrical characteristics, the results of only one Al/PIN SBD, as a typical device, is introduced in this work. For a metal/semiconductor (M/S) or metal/polymer (M/P) contact, the current through a SBD can be given by.[8,9]

$$I = I_0 \exp\left(\frac{qV}{nkT}\right)\left[1 - \exp\left(\frac{-qV}{k_B T}\right)\right] \quad (1)$$

where I_0 is the reverse saturation current and is equal to

$$I_0 = AA^* T^2 \exp\left(-\frac{q\Phi_{B0}}{k_B T}\right) \quad (2)$$

where Φ_{B0} is the zero-bias barrier height, A is the circular diode area ($A = \pi r^2$), A^* is the effective Richardson constant, n is an ideality factor, T is the absolute temperature in Kelvin, k_B is the Boltzmann's constant, and V is the applied forward bias voltage.

The semilogarithmic forward bias I–V plots of the Al/PIN SBD in the temperature range of 140–400 K are shown in Figure 1 as decimal (a) and semilogarithmic (b), respectively. As can be seen in Figure 1(b), the ln I–V plots deviated from linearity at high forward bias voltages due to effect of series resistance. Although the R_s is significant especially in the downward curvature of the forward bias I–V characteristics, the density of surface states N_{ss} is effective in both inversion and depletion range; and their distribution profile changes from region to region in the band gap of PIN.

The reverse saturation current I_0 values were obtained by extrapolating the linear portion of the forward bias ln I–V plot [Fig. 1(b)] to the intercept point on the current axis at zero-bias ($V = 0$) and the zero-bias barrier height Φ_{B0} values were calculated using eq. (2). The values of ideality factor n were calculated from the slopes of ln I–V plots in the linear region ($0.1 \leq V \leq 0.6$ V) and can be written [using eq. (1)] as;

$$n = \frac{q}{k_B T}\left(\frac{dV}{d\ln(I)}\right) \quad (3)$$

The changes in I_0, n, and Φ_{B0} with temperature are given in Table I. The calculated values of I_0, n, and Φ_{B0} were found to be strongly temperature dependent. The experimentally obtained values of I_0, n, and Φ_{B0} for the Al/PIN SBD were changed from 6.2×10^{-10} A, 9.80, and 0.375 eV (at 140 K) to 2.4×10^{-6} A, 2.69, and 0.85 eV (at 400 K). Such a behavior of ideality factor has been attributed to particular distribution of interface states and insulator layer between Al and PIN.[13–16]

These values of Φ_{B0} calculated from forward bias I–V characteristics have shown an unusual behavior such that it increases with increasing temperature. Such behavior of ideality factor and barrier height can be explained by means of the bias dependence of saddle-point potential of an inhomogeneous barrier height.[15–19] Therefore, the current through the

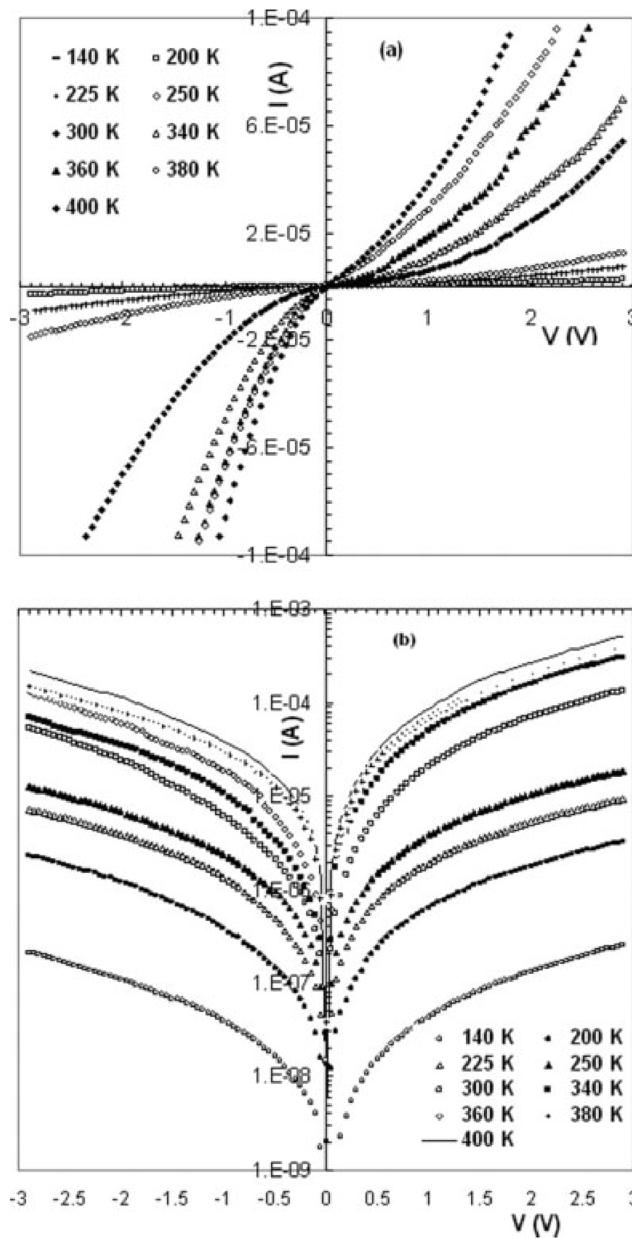

Figure 1 The temperature dependence of (a) the $I-V$ and (b) ln $I-V$ characteristics of Al/PIN SBD.

diode will flow preferentially through the lower barriers in the potential distribution.[15–18]

The values of ideality factor n are found to be increasing, whereas the Φ_{B0} decreases with decreasing temperature (Fig. 2). The high values of the ideality factor were shown a deviation from pure thermionic emission (TE) theory in the current-conduction mechanism,[19–22] which indicates a nonideal behavior. As explained in the literature by various researchers[15–19] because the current transport across the diode is a temperature-activated process, electrons at low temperatures are able to surmount the lower barriers. Therefore, the current transport will be dominated by the current flowing through the patches of lower Schottky barrier heights, leading to a larger ideality factor. In other words, more and more electrons have sufficient energy to overcome the height barrier build-up with increasing temperature and bias voltage.

TABLE I
The Values of Various Electrical Parameters for the Al/PIN SBD Determined from the Forward Bias ln I–V Characteristics in the Temperature Range of 140–4000 K

T(K)	I_0(A)	n	$\Phi_B(I–V)$ (eV)
140	6.20×10^{-10}	9.80	0.375
200	2.10×10^{-8}	6.12	0.487
225	6.48×10^{-8}	5.15	0.530
250	1.35×10^{-7}	4.35	0.578
300	3.80×10^{-7}	3.50	0.676
340	8.80×10^{-7}	3.13	0.749
360	1.60×10^{-6}	2.98	0.778
380	2.00×10^{-6}	2.80	0.818
400	2.40×10^{-6}	2.69	0.850

For the evaluation of the Schottky barrier height, one may also make use of a Richardson plot of the saturation current. Using the saturation current [eq. (2)], for the evaluation of E_a the Richardson plot can be drawn from the following equation.[20,21]

$$Ln\left(\frac{I_0}{T^2}\right) = \ln(AA^*) - \frac{qE_a}{k_B T} \tag{4}$$

A conventional ln (I_0/T^2) vs. $1/T$ plot is shown in Figure 3. From the slope of this curve, $E_a = 0.115$ eV was calculated for the Al/PIN SBD.

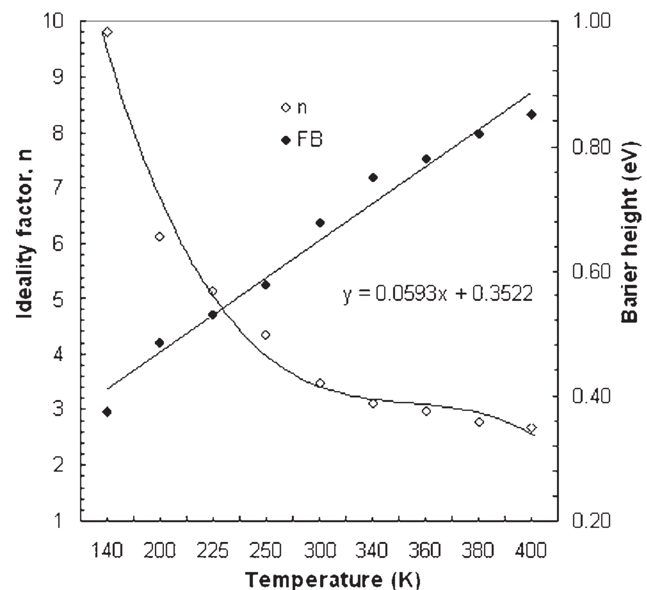

Figure 2 Temperature dependence of Φ_B and n obtained from forward bias $I-V$ characteristics for the Al/PIN SBD.

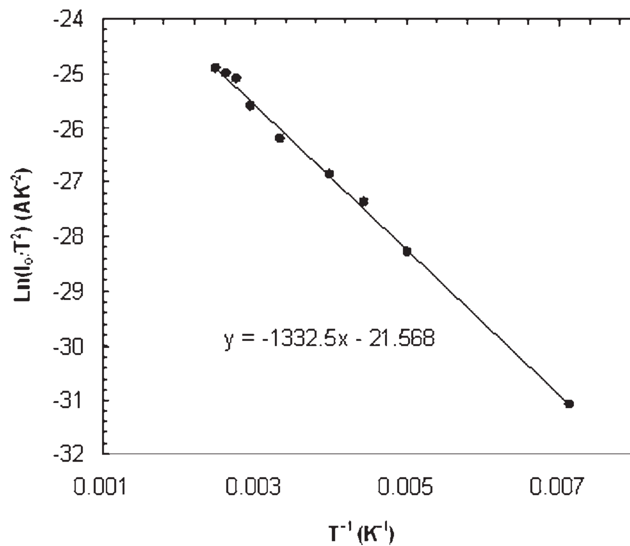

Figure 3 ln (I_0/T^2) vs. $1/T$ plot for Al/PIN SBD.

The temperature dependence of *C–V* and *G/ω–V* characteristics

The advantage of lowering temperature is the ability to measure surface states, which are not normally accessible at room temperature. Because the time constant of the states is lowered with temperature so that states are brought into the range of measured frequencies between 500 kHz–1 MHz; and Fermi level moves closer to the majority carrier band edge so that states at different energies in the band are probed.[23] Therefore, the temperature-dependent *C–V* and *G/ω–V* characteristics of Al/PIN SBD was measured in the temperature range of 140–400 K at 500 kHz.

The real series resistance of devices can be subtracted from the measured capacitance (C_{ma}) [Fig. 4(a)] and conductance (G_{ma}) [Fig. 4(b)] in strong accumulation region at high frequency (≈500 kHz).[24–28] According to Nicollian and Brews,[24] at sufficiently high frequency, to determine series resistance R_s, the devices are biased into strong accumulation, series resistance can be obtained as:

$$R_s = \frac{G_{ma}}{G_{ma}^2 + (\omega C_{ma})^2} \qquad (5)$$

where C_{ma} and G_{ma} represent the measured capacitance and conductance in strong accumulation region, respectively. Figure 4(a,b) show the 500 kHz *C–V* and *G/ω–V* characteristics of the Al/PIN SBD measured at various temperatures with an oscillator level of 40 mV peak to peak. Over the voltage range studied (–10 V, +15 V), both capacitance and conductance were observed to decrease with increasing temperature. Figure 4(a) indicates that the values of *C* give a peak especially at high temperature, shifting to reverse bias region with increasing temperature. It was also realized that the change in the temperature have effects on the values and positions of these anomalous peaks. Figure 4(b) shows *G/ω–V* characteristics of Al/PIN SBD at various temperatures. The measured accumulation capacitance (C_{ma}) increase with temperature, which implies for the parallel circuit mode that the series resistance (R_s) decreases with temperature.[24,29]

The values of R_s obtained from the dispersion in the accumulation capacitance and conductance according to eq. (5) is given in Figure 5. The values of R_s observed to decrease with increasing temperature. This behavior of R_s is believed to result from the factor responsible for increase of ideality factor *n* and lack of free carrier concentration at low temperature.[26]

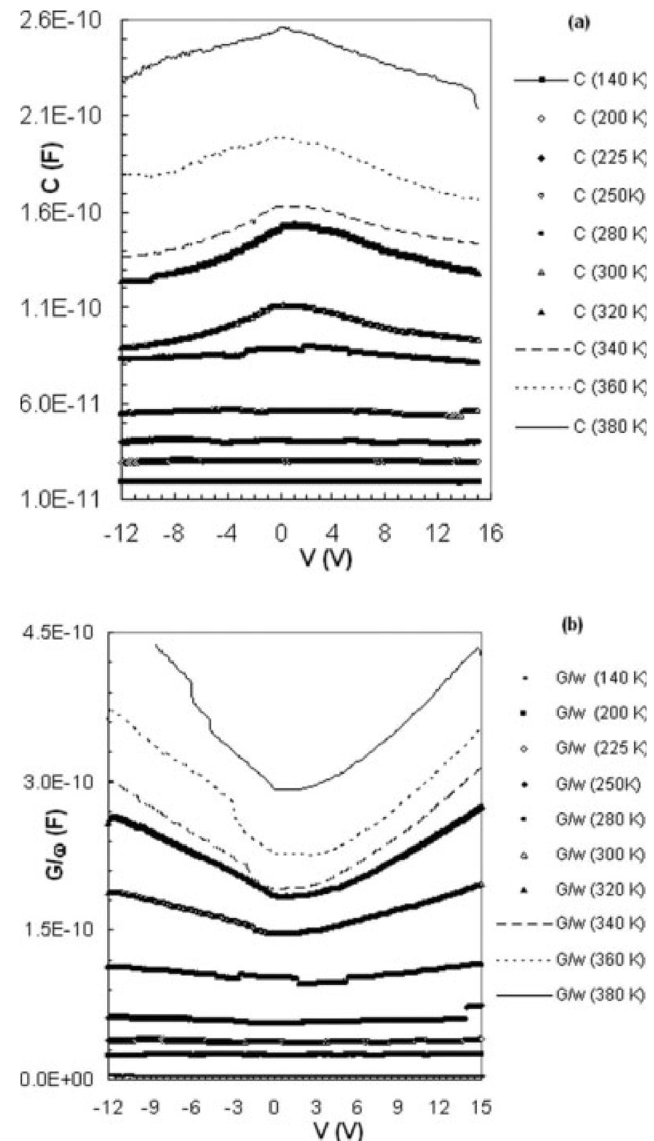

Figure 4 (a) The *C–V* and (b) *G/ω–V* characteristics of Al/PIN SBD at various temperatures.

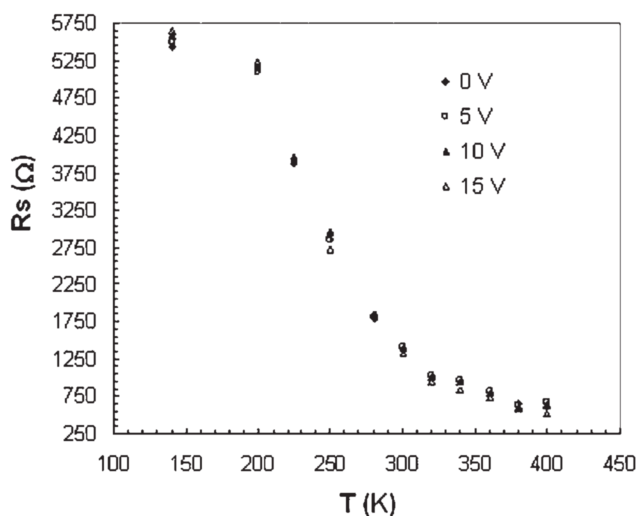

Figure 5 The temperature dependence of the series resistance at various forward bias for Al/PIN SBD at 500 kHz.

In general, conducting polymers behave as semiconductors in the temperature dependence of σ_{ac}.[30,31] The $\sigma_{ac}C$–V and σ_{ac}–T plots of the Al/PIN SBD at various temperatures are shown in Figures 6 and 7, respectively. The values of conductivity increased with increasing temperature. The variation of σ_{ac} was remarkably high at high temperatures, but it was very small at low temperatures. This behavior of conductivity with increasing temperature is typical of semiconductor behavior. There have been a several reports in the literature,[31–33] in which the temperature-dependent conductivity data of conducting polymers have been fitted to the Arrhenius equation of conductivity:

$$\sigma_{ac} = \sigma_0 \exp\left(\frac{-qE_a}{kT}\right) \qquad (6)$$

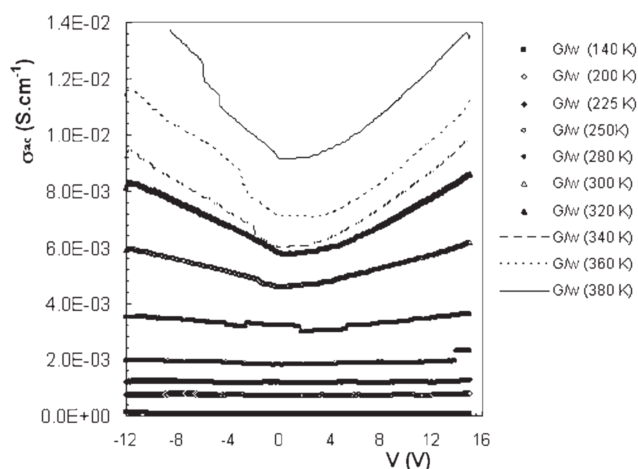

Figure 6 The σ_{ac} vs. V plot of Al/PIN SBD at various temperatures.

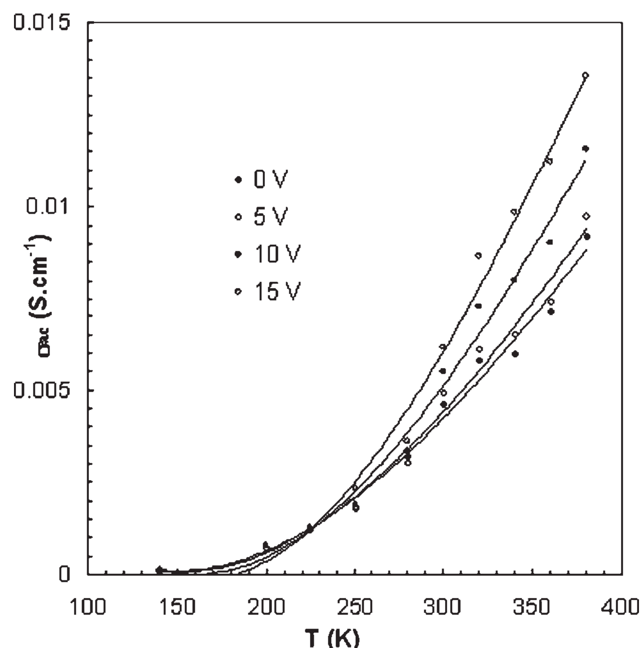

Figure 7 Temperature dependence of σ_{ac} at various forward bias for Al/PIN SBD at $f = 500$ kHz.

A plot of ln σ_{ac} vs. $1/T$ is a straight line (Fig. 8). The E_a values of Al/PIN SBD obtained from the slope of ln σ_{ac}–$1/T$ plots are 0.088, 0.090, 0.094, and 0.097 eV for the values of forward bias of 0, 5, 10, and 15 V, respectively.

The electrical transport mechanism may be due to Mott variable range hopping.[31–34] In this model, the conductivity is treated as temperature-activated hopping from center to center. The lack of ordering in amorphous conducting polymers is expected to produce localized states, which can move by thermally

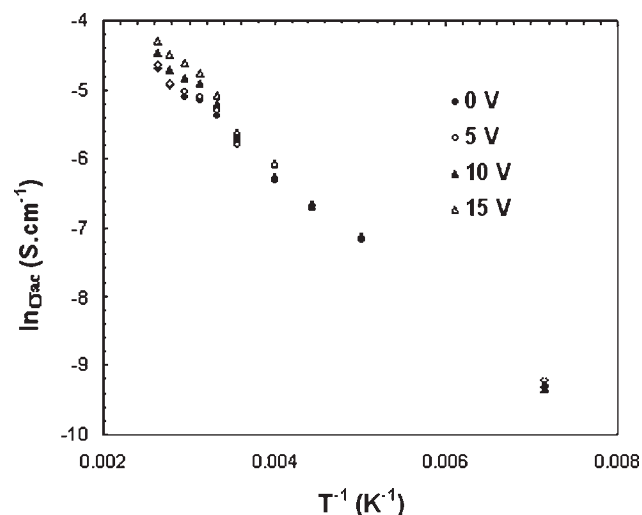

Figure 8 The Arrhenius plot of σ_{ac} at various forward bias of the Al/PIN SBD at $f = 500$ kHz.

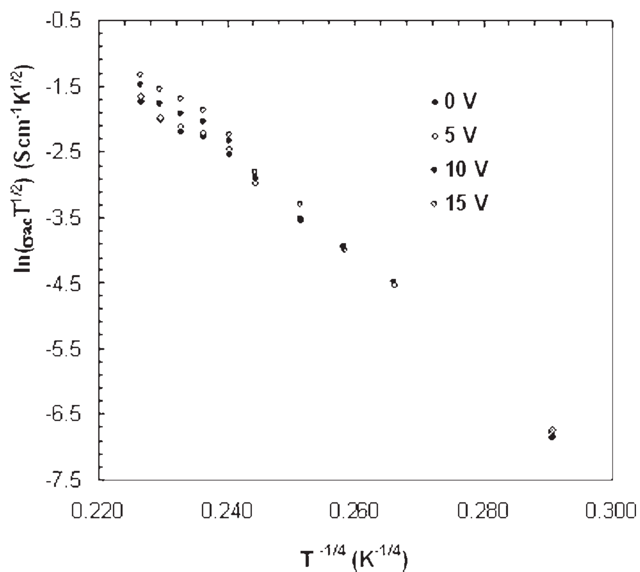

Figure 9 The Mott plot of the σ_{ac} at various forward bias for the Al/PIN SBD at $f = 500$ kHz.

activated hopping to another localized interface states and conduction occurs through variable range hopping of the electron between these localized interface states. The Mott model[34] that defines the relation between conductivity and temperature is:

$$\sigma_{ac} = K_0 T^{-1/2} \exp\left[-\left(\frac{T_0}{T}\right)^{1/4}\right] \quad (7)$$

$$T_0 = \frac{16\alpha^3}{k_B N(E_F)} \quad (8)$$

$$K_0 = 0.39\left[\frac{N(E_F)}{\alpha k_B}\right]^{1/2} \nu_0 e^2 \quad (9)$$

where $\alpha^{-1}$is the decay length of the localized state; ν_0 is the hopping attempt frequency; $N(E_F)$ is the density states at the Fermi energy level; e is the electronic charge; T_0 is the Mott characteristic temperature, and K_0 is the Mott characteristic conductivity parameter.

The conductivity data obtained for PIN in the temperature range of 140–400 K are used to construct the Mott plot (Fig. 9). The Mott parameters of T_0 (3.8 $\times$ 10^7 K) and K_0 (1.08 $\times$ 10^7 $Scm^{-1}K^{1/2}$) are obtained from the slope and intercept of the graph, respectively. Substituting these values in equations and assuming a value of 6 $\times$ 10^{12} s^{-1} for ν_0,[31] the decay length α^{-1} and $N(E_F)$ are estimated to be 8.74 Å and 1.27 $\times$ 10^{20} eV^{-1} cm^{-3}, respectively.

CONCLUSIONS

The temperature-dependent reverse and forward bias I–V, C–V, and G/ω–V characteristics of the Al/PIN SBD were measured in the temperature range of 140–400 K. The I–V characteristics of Al/PIN SBD shown almost rectification behavior, but the values of reverse bias saturation current (I_0) and n were high. These behaviors have been attributed to particular distribution of barrier heights, barrier inhomogeneity, and interface states localized at the Al/PIN SBD. Experimental results shown that both the values of C, G/ω, and σ_{ac} were quite sensitive to temperature, especially at relatively high temperature and behavior was attributed to the thermal restructuring and reordering of the interface. Also, the variation of C, G/ω, and σ_{ac} was remarkably high at high temperature, but it was very small at low temperature. The analysis of experimental data shown that hopping of carriers between localized interface states is the dominant conduction mechanism.

References

1. Abthagir, P. S.; Saraswathi, R. Org Electron 2004, 5, 299.
2. Gupta, R. K.; Singh, R. A. Mat Sci Semicon Proces 2004, 7, 83.
3. Abthagir, P. S.; Saraswathi, R. J. Mater Sci Mater Electron 2004, 15, 81.
4. Gupta, R. K.; Singh, R. A. Compos Sci Techn 2005, 65, 677.
5. Lee, Y. S.; Park, J. H.; Choi, J. S. Opt Mater 2002, 21, 433.
6. Abthagir, P. S.; Saraswathi, R. J. Appl Polym Sci 2001, 81, 2127.
7. Campos, M.; Bulhoes, L. O. S.; Lindino, C. A. Sens Actuators 2000, 87, 67.
8. Zhu, M.; Cui, T.; Varahramyan, K. Microelectron Eng 2004, 75, 269.
9. Aydogan, S.; Saglam, M.; Turut, A. Polymer 2005, 46, 563.
10. Singh, R.; Srivastava, D. N.; Singh, R. A. Synth Met 2001, 121, 1439.
11. Aydogan, S.; Saglam, M.; Turut, A. Polymer 2005, 46, 10982.
12. Cakar, M.; Turut, A.; Onganer, Y. J Solid State Chem 2002, 168, 168.
13. Crowell, C. R.; Sze, S. M. Solid State Electron 1966, 9, 1035.
14. Card, H. C.; Rhoderick, E. H. J. Phys D Appl Phys 1971, 4, 1589.
15. Pakma, O.; Serin, N.; Serin, T.; Altindal, S. Semicond Sci Technol 2008, 23, 105014.
16. Altindal, S.; Dokme, I.; Bulbul, M. M.; Yalcin, N.; Serin, T. Microelektron Eng 2006, 83, 499.
17. Mönch, W. J. Vac Sci Technol 1999, 17, 1867.
18. Karatas, S.; Altindal, S.; Turut, A.; Ozmen, A. Appl Surf Sci 2003, 217, 250.
19. Schmitsdorf, R. F.; Kampen, T. U.; Mönch, W. J. Vac Sci Technol 1997, 15, 1221.
20. Sze, S. M.Physics of Semiconductor Devices, 2nd ed.; Wiley: NY, 1981.
21. Rhodecik, E. H.; Williams, R. H.Metal-Semiconductor Contacts, 2nd ed.; Clarendon Press: Oxford, 1988.
22. Karatas, S.; Altindal, S.; Cakar, M. Phys B 2005, 357, 386.

23. Kwa, K. S. K.; Chattopadhyay, S.; Jankovic, N. D.; Olsen, S. H.; Driscoll, L. S.; Neill, A. G. O. Semicon Sci Techn 2003, 18, 182.
24. Nicollian, E. H.; Brews, J. R.MOS Physics and Technology; Wiley: NY, 1982.
25. Kanbur, H.; Altindal, S.; Tataroglu, A. Appl Surf Sci 2005, 252, 1732.
26. Bulbul, M. M.; Zeyrek, S.; Altindal, S.; Yuzer, H. Microelectron Eng 2006, 83, 577.
27. Altindal, S.; Tataroğlu, A.; Dokme, I. Sol Energy Mater Sol Cells 2005, 85, 343.
28. Tekeli, Z.; Altindal, S.; Cakmak, M.; Ozcelik, S.; Ozbay, E. Microelecton Eng 2008, 85, 2316.
29. Altindal, S.; Kambur, H.; Yucedag, I.; Tataroglu, A. Microelectron Eng 2008, 85, 1495.
30. Roth, S. Ind J Chem 1994, 33, 453.
31. Abthagir, P. S.; Dhanalakshmi, K.; Saraswathi, R. Synth Met 1998, 93, 1.
32. Abthagir, P. S.; Saraswathi, R.; Sivakolunthu, S. Thermocimica Acta 2004, 411, 109.
33. Abthagir, P. S.; Saraswathi, R. Thermocimica Acta 2004, 424, 25.
34. Mott., N. F. Adv Phys 1967, 16, 49.